Journal of Materials Chemistry C

Fluorographenes via Thermal Exfoliation of Graphite Oxide in SF6, SF4 and MoF6 atmospheres

Journal:	*Journal of Materials Chemistry C*
Manuscript ID:	TC-ART-02-2014-000395.R1
Article Type:	Paper
Date Submitted by the Author:	21-Apr-2014
Complete List of Authors:	Poh, Hwee Ling; Nanyang Technological University, Chemistry and Biological Chemistry Sofer, Zdenek; Institute of Chemical Technology, Prague, Department of Inorganic Chemistry Klimova, Katerina; Institute of Chemical Technology, Prague, Department of Inorganic Chemistry Pumera, Martin; Nanyang Technological University, Chemistry and Biological Chemistry

Journal Name

RSCPublishing

ARTICLE

Fluorographenes *via* Thermal Exfoliation of Graphite Oxide in SF_6, SF_4 and MoF_6 atmospheres

Cite this: DOI: 10.1039/x0xx00000x

Hwee Ling Poh[a], Zdeněk Sofer[b], Kateřina Klímová[b] and Martin Pumera[a]*

Received 00th January 2012,
Accepted 00th January 2012

DOI: 10.1039/x0xx00000x

www.rsc.org/

Functionalization of graphene with heteroatoms is of paramount interest. Doping of graphene materials with electron withdrawing groups leads to the opening of the band gap which further results in a change of its electronic and electrochemical properties. Fluorine exhibits the largest electronegativity and thus it is expected that fluorographenes will have significantly different properties from graphene. Fluorinated graphene was prepared by a scalable method using thermal treatments (at different temperatures) or microwave plasma exfoliation of graphite oxides (prepared *via* chlorate or permanganate routes) in atmospheres containing SF_6, SF_4 or MoF_6 fluorination agents. We characterized the resulting fluorographenes by scanning electron microscopy, Raman spectroscopy, X-ray photoelectron spectroscopy, combustible elemental analysis and cyclic voltammetry. It was observed that with increasing fluorine content the heterogeneous electron transfer rates increases. The scalable fluorination of graphene with relatively low-toxic agents which yields high-performance electrochemical materials should find many applications in electrochemical devices, such as sensors or supercapacitors.

Introduction

Graphene, a single atomic layer of carbon atoms have fascinated many researchers with its numerous excellent advantages such as its mechanical, optical, electrical and electrochemical properties. [1, 2] Hence, intensive research works have been carried out where graphene were utilized in important future applications such as supercapacitors and biosensors.[2,3] Despite many advantageous properties, certain characteristics of graphene such as zero band gap have proved the material to be a challenge for some applications.[4] Therefore, intensive studies were carried out to dope/derivatize graphene with various elements in an attempt to improve the disadvantages that graphene has posed. Researches have previously showed that derivatization/doping of graphene is possible with elements such as halogens (Cl, Br, I)[5], boron[6], hydrogen[7], sulphur[8-10], nitrogen[11] and phosphorus.[12] Halogen atoms (together with hydrogen) offer simple and controllable functionalization of graphene, as they bond to carbon structure only *via* uncomplicated single C-X bond; this is in contrary of several functional groups the other heteroatoms such as N, P, S or even B can create. Halogen doping offers way to tune the band gap via either choice of the halogen5 or via halogen coverage of graphene sheets. Among several of these materials, fluorinated graphene has been widely known to be one of the more stable doped graphene materials to be synthesized as compared to its other doped counterparts.[13] This property is especially crucial in applications where stability of the materials is a major concern as the reliability and effectiveness of the device is directly affected by the quality of the material. The production of fluorinated graphene was often achieved with reagents such as xenon difluoride (XeF_2)[14-17], Ar/F_2[18], sulfur hexafluoride (SF_6)[19], fluoropolymers[20] or tetrafluoromethane (CF_4).[21-23] Since XeF_2 and F_2 are highly toxic, expensive and/or corrosive, we have focused on the fabrication of fluorinated graphenes via synthesis using SF_6 and other less commonly used fluorine sources such as sulfur tetrafluoride (SF_4) and molybdenum hexafluoride (MoF_6). Additionally, we have focused on methodology which is able to be scalable, yielding grams or kilograms of the material. For this reason we used method based on thermal exfoliation of graphite oxide, which can be prepared in gram/kilogram quantities, in SF_6, SF_4 or MoF_6 atmospheres. This is in comparison with previous methods where only individual monolayers of graphene were functionalized with fluorine.[16-21] Because it has been previously shown that composition of graphite oxide, that is, whether it is prepared by chlorate (Staudenmaier or Hofmann) or permanganate (Hummers) routes exhibits strong influence on the incorporation of sulphur and phosphorus, herein we will also study the influence of graphite oxide origin upon fluorine incorporation as well. We have characterized the products

with combustible elemental analysis, X-ray photoelectron spectroscopy, Raman spectroscopy and will attempt to display how fluorine influences the heterogeneous electron transfer in resulting fluorographenes.

Results and Discussion

We have first prepared graphite (GO) oxides from graphite using various methods, chlorate (Staudenmaier (ST) or Hofmann(HO)) and permanganate (Hummers (HU)) based. Consequently, we exfoliated the graphite oxide in atmosphere of fluorination agent, such as SF_6, SF_4 and MoF_6 (Scheme 1). Resulting fluorinated materials were labelled in accordance to their methods of preparation, which includes the type of graphite oxide and fluorination agent source used and the temperature, e.g. HO-F: [SF_6/800°C]. In-depth characterization of the materials was performed using an array of different techniques to determine the properties of each material. A range of methods that were employed includes scanning electron microscopy (SEM), X-ray photoelectron spectroscopy (XPS), combustible elemental analysis, Raman spectroscopy and an electrochemical cyclic voltammetry technique. The results obtained were also further compared against standards such as non-fluorinated thermally reduced graphene oxides (TRGOs) synthesized from Hummers, Staudenmaier and Hofmann methods. The standard materials are labelled as HU, ST and HO for materials produced from Hummers, Staudenmaier and Hofmann methods respectively. Such a comparison allows a clearer understanding of how chemical treatments with fluorine sources influence the properties of graphene oxides.

We compare Hummers, Staudenmaier and Hofmann method of synthesis of graphite oxide due to the fact that there were previously shown to have strong effect on incorporation of heteroatom in the graphene.[10] As such, we will investigate the properties of fluorinated graphene synthesized using three different fluorine sources: SF_6, SF_4 and MoF_6. SEM images of HU-F: [SF_6/800°C], HU-F: [SF_4/800°C] and HU-F: [MoF_6] are as shown in Figure 1 where the materials were observed at x50,000, x10,000, x6,000 and x370 magnifications. XPS results have shown that HU-F: [SF_6/800°C] have the highest fluorine content which will be further discussed later. As such, similar treatment methods have been employed for HO-F and ST-F (where HO-F stands for Hofmann method prepared graphite which was thermally exfoliated and fluorinated by one of the agents; ST-F stands for similar material originating from Staudenmaier method prepared GO) to observe if identical results were also observed for these materials. SEM images for these materials are as shown in Figure 1. Fluorination method was also performed in microwave plasma graphene oxide (MW-F: [SF_6]) and reaction temperature was also further varied for

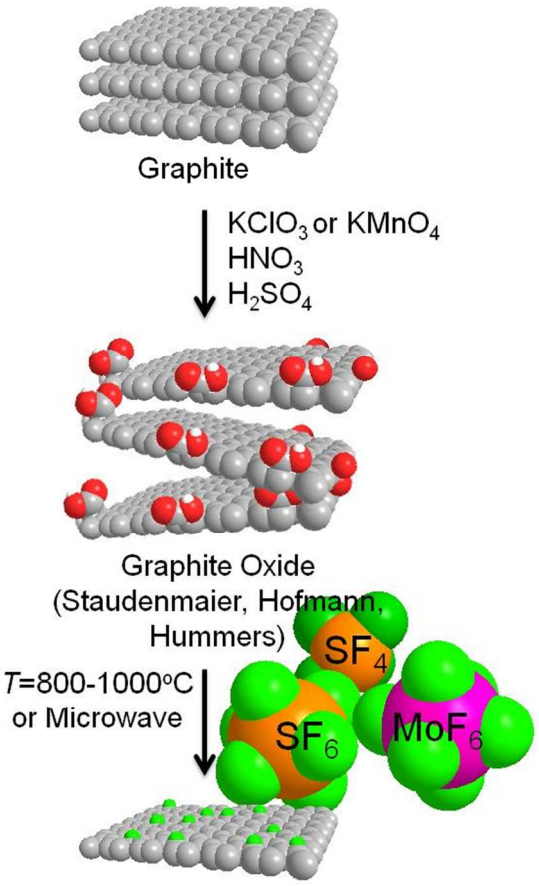

Scheme 1. Schematic fluorination of graphene.

the same fluorine source (ST-F: [SF_6/1000°C]). The SEM images for these materials and the control materials (HU, HO and ST-GO exfoliated in the inert atmospheres) are also shown in Figure 1. It can be observed that all the fluorinated materials and their standards display images that are typical of fully exfoliated thermally reduced graphene oxides. This implies that all fluorinated graphenes are exfoliated during the synthesis process. One should note that SF_6 is completely safe gas, used in industry as insulator gas in high voltage insulation. SF_4 and MoF_6 are highly toxic; MoF_6 is low boiling point liquid (b.p, 36 ^{o}C) which is prone to hydrolysis by humidity.

Further surface properties such as the density of defects were also investigated through Raman spectroscopy. The amount of defects in a material is determined by the intensities of the D band and G band at 1350 cm^{-1} and 1560 cm^{-1} respectively. D band represents the presence of sp^3 defects found in the pristine sp^2 lattice while G band is derived from the pristine sp^2 graphene network lattice. Therefore, calculation of the D/G ratio from the intensities of the two peaks provides insight on the density of defects present in each material. The Raman spectrum of the individual materials are as shown in Figure 2. In the comparison between Hummers materials, HU-F: [SF_6/800°C] showed a D/G ratio of 1.16, HU-F: [SF_4/800°C] has a D/G ratio of 1.17 followed by HU-F: [MoF_6] of 0.93.

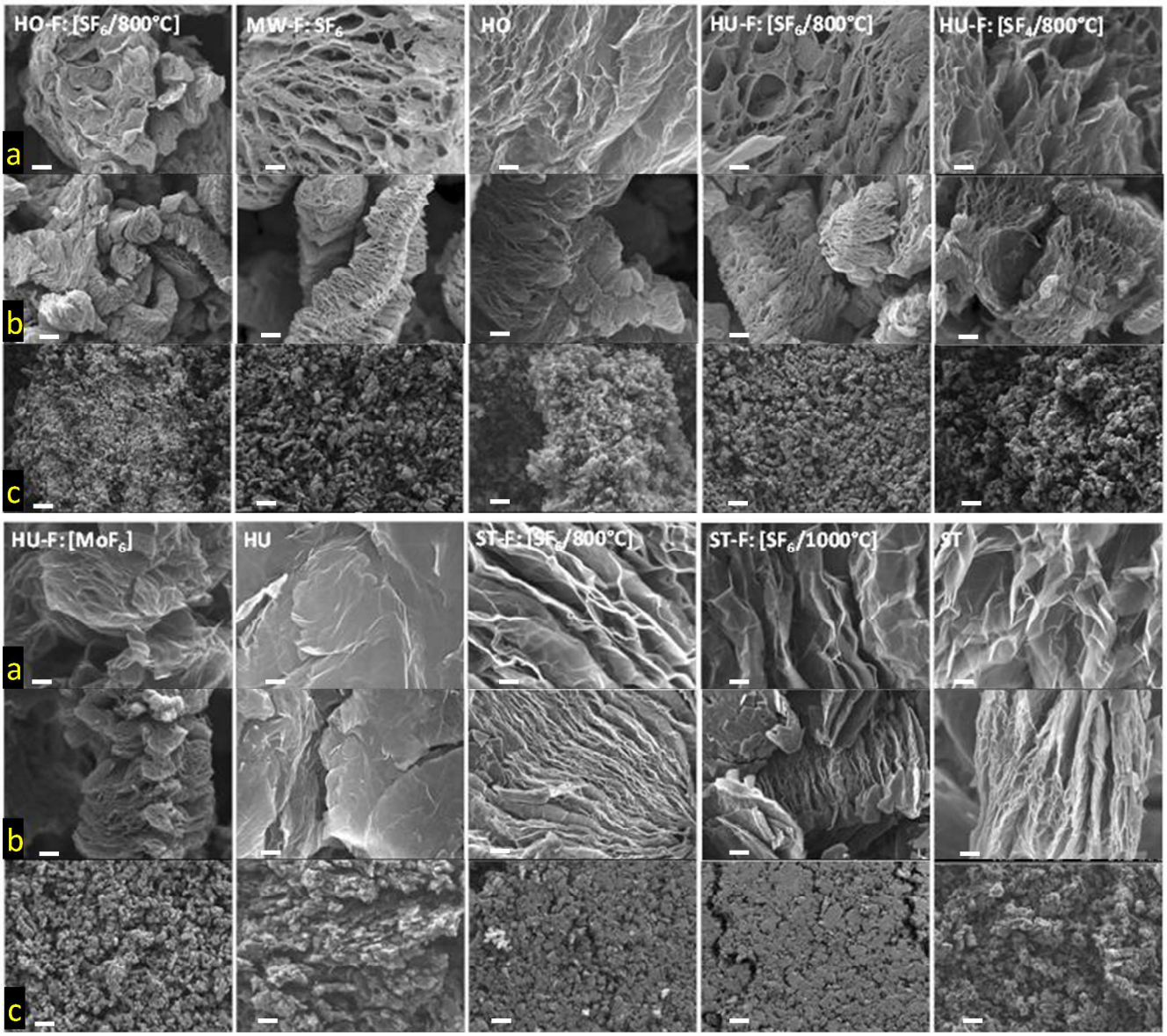

Figure 1. Scanning electron micrographs for fluorinated graphenes. Scale bars of (a) 200 nm, (b) 1μm and (c) 25 μm.

HO-F: [SF_6/800°C] was observed to have a D/G ratio of 1.14 while MW-F: [SF_6] was found to have a density of defects of 0.95. Similarly, ST materials were treated with the same fluorine source at the same temperature to give ST-F: [SF_6/800°C]. ST-F: [SF_6/800°C] was observed to possess a D/G ratio of 0.86 while ST-F: [SF_6/1000°C] has a ratio of 0.59. The materials used as standards for comparison are HU, HO and ST which were found to possess ratios of 0.97, 1.09 and 0.77 respectively. The D/G ratios each material are presented as a bar graph for comparison as shown in Figure 2, D. It can be easily observed that materials doped using SF_6 as the source at 800°C usually possess the highest D/G ratio as compared to their counterpart materials. It was also found that all materials dopedwith SF_6 or SF_4 as the fluorine source have higher D/G ratios as compared to their respective standards with the exception of ST-F: [SF_6/1000°C]. For standard deviation of D/G ratios see Table S-1. This indicates that doping of the materials with fluorine leads to the introduction of defects onto the surface where earlier reports have shown similar findings of higher D/G ratios after fluorination.[14] The average crystallite size of the materials can also be calculated using the peaks' intensities and the following equation[24]:

$$L_a = 2.4 \times 10^{-10} \times \lambda_{laser}^{\ 4} \times I_G/I_D$$

where L_a is the average crystallite size of the material, I_G and I_D denotes the intensity of the G and D peaks respectively while λ_{laser} is the wavelength of the laser used in nm. The L_a calculated for the materials are 14.44 nm for HU-F: [SF_6/800°C], 14.35 nm HU-F: [SF_4/800°C] and 18.09 nm for HU-F: [MoF_6]. HO-F: [SF_6/800°C] has a value of 14.71 nm, MW-F: [SF_6] has a value of 17.71 nm. ST-F:

[SF_6/800°C] has a value of 19.59 nm while ST-F: [SF_6/1000°C] has a value of 28.50 nm. The standards have the following sizes of 17.30 nm, 15.41 nm and 21.70 nm for HU, HO and ST respectively. Similarly, materials doped using SF_6 at 800°C usually have the smallest crystallite size as compared to their counterparts.

In addition we measured micro-photoluminescence spectra using 325 nm a 532 nm laser excitation. The spectra for both excitation wavelengths are shown on Figure SI 1. No luminescence was observed for UV excitation up to 500 nm. Weak band around 341 nm and 360 nm originate from Raman scattering (D, G and 2D bands). For the UV excitation on samples HO-F:[SF_6/800°C] and HU-F:[SF_4/800°C] exhibit luminescence with maximum at 540 nm and 730 nm, respectively. For the green laser excitation (532 nm) we observed strong luminescence in NIR-IR region with maxima in the range of 970 – 1000 nm. This was observed for samples originated from HO and HU graphene except HU-F: [MoF_6] sample. This correspond to band-gap energy of 1.2 – 1.3 eV. The line observed at 685 nm on some samples originates from laser plasma line. In addition to photoluminescence the absorbance of F doped graphene suspension were measured. Absorbance spectra are shown on figure SI 2. The absorbance is constant in the range of 1100 – 300 nm with subsequent decrease for the wavelength below 300 nm. No correlation with photoluminescence measurement can be observed in comparison due to the high absorption coefficient and heterogeneous nature of graphene suspensions.

Surface elemental composition of the materials was determined using X-ray photoelectron spectroscopy (XPS). A wide-range scan was performed on the materials as shown in Figure 3, A, B and C. All materials showed C 1s peak at 284.5 eV, O 1s peak at 534 eV as the major peaks. F 1s peak at approximately 688 eV could be clearly observed for all fluorinated materials as denoted in Figure 3. The relative amount (%) of the total counts for F 1s for each material compared to carbon content was computed and shown in the bar graph as shown in Figure 3, D. Most commonly synthesized HU materials are fluorinated to give HU-F: [SF_6/800°C] with the highest F 1s composition of 1.92% followed by HU-F: [SF_4/800°C] with 0.53% HU-F: [MoF_6] with 0.26%. As such, similar treatment methods were applied to HO material to give HO-F: [SF_6/800°C] which possessed 0.59% of F 1s on the material's surface. Microwave graphene was also fluorinated with SF_6 to give 1.05% of fluorine. ST-F: [SF_6/800°C] contains of 4.25% based on F 1s data while ST-F: [SF_6/1000°C] recorded a total of 0.49% of F 1s. It can be clearly seen that materials treated with SF_6 at 800°C have the highest F 1s % content as compared to their counterpart materials. This observation is in agreement with the Raman results obtained earlier where graphene oxides that are fluorinated using SF_6 at 800°C usually have the highest density of defects as compared to the other materials. The degree of oxidation of the materials can be investigated through the calculation of C/O ratio using the intensities of the C 1s peak and the O 1s peak. The C/O ratios of the materials are then presented as a bar graph for comparison as shown in Figure 3, E. HU-F: [SF_6/800°C] has a C/O ratio of 17.77 followed by HU-F: [SF_4/800°C] with 14.15 and HU-F: [MoF_6] with 14.29. HO-F: [SF_6/800°C] was observed to have a ratio of 17.97 while microwave graphene fluorinated with SF_6 has a C/O value of 9.75. At the same time, ST-F: [SF_6/800°C] possessed a C/O ratio of 25.06 while ST-F: [SF_6/1000°C] has a value of 24.68. The standard materials that are non-fluorinated for comparison are calculated to have ratios of 19.28, 18.23 and 27.10 for HU, HO and ST respectively. This shows that most non-fluorinated reduced graphene oxides are less oxidized as compared to their fluorinated counterparts except for ST. This indicates that fluorination of the materials usually resulted in lesser oxygen containing groups being removed from the materials as compared to the exfoliation process for the control materials. Similarly, the extent of fluorination can also be determined through the calculation of the F/C ratio as shown in the bar graph in Figure 3, F. HU-F: [SF_6/800°C] was observed to possess a F/C ratio of 0.022 followed by HU-F: [SF_4/800°C] with 0.006 and HU-F: [MoF_6] with 0.003. HO-F: [SF_6/800°C] shows a value of 0.007 and fluorinated microwave graphene has a value of 0.012. ST-F: [SF_6/800°C] has a F/C ratio of 0.047 while ST-F: [SF_6/1000°C] is 0.005. It can be easily observed that the higher is the C/O ratio (i.e. the less oxidized) of the starting material, the more fluorine atoms are introduced onto the surface of the material during fluorination. Hence, it was concluded that ST-F: [SF_6/800°C] has the highest percentage of fluorine on the surface of the material as compared to HO-F: [SF_6/800°C] and HU-F: [SF_6/800°C]. This results show that fluorination using SF_6 as the source at 800°C still provides the highest fluorine content regardless of the graphene (HU, HO, ST) starting material used.

The percentage content of each major element (nitrogen, carbon, hydrogen, fluorine and oxygen) can be obtained through CHN/O combustion elemental analysis. The result for each material is as summarized in Table 1. It can be observed that ST-F: [SF_6/800°C] has the highest atomic. % fluorine (at. % F) content of 2.40 followed by HU-F: [SF_6/800°C] of 2.21 %. HU-F: [MoF_6] was found to possess the lowest at. % F amount of just 0.84. This results support the earlier findings on the % of F 1s content in XPS where ST-F: [SF_6/800°C] has the highest concentration of fluorine on the surface, followed by HU-F: [SF_6/800°C]. Similarly, HU-F: [MoF_6] has the lowest amount of fluorine attached onto the surface of the material. We wish to show here that the different graphite oxides lead into the different fluorination yields.

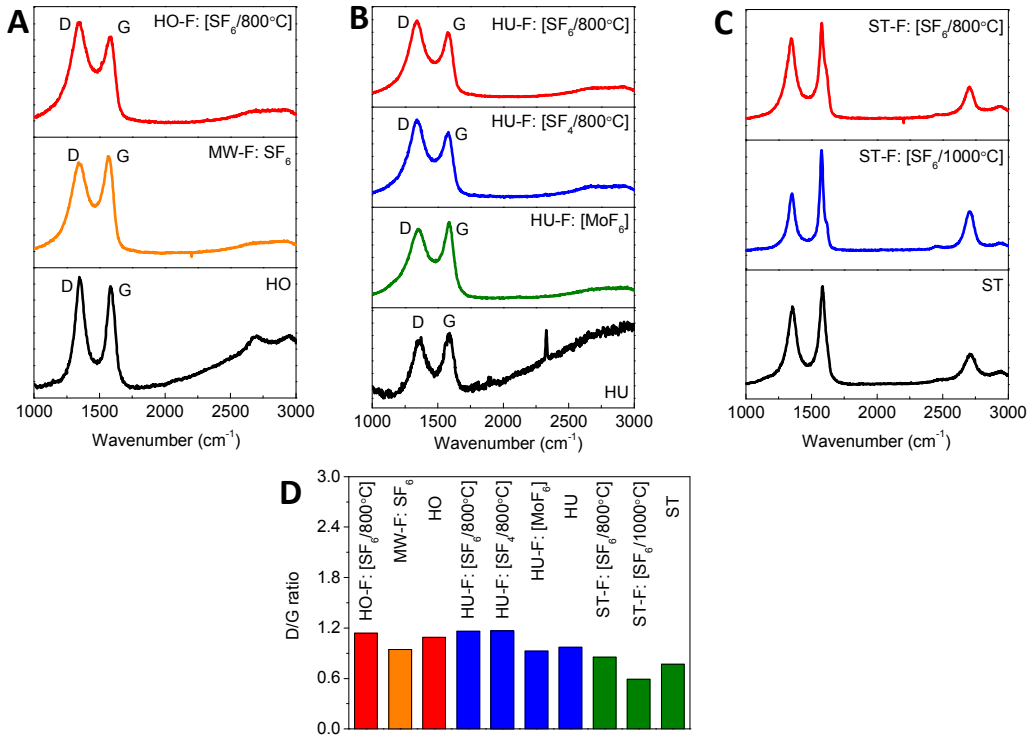

Figure 2. Raman spectra of fluorinated graphenes.

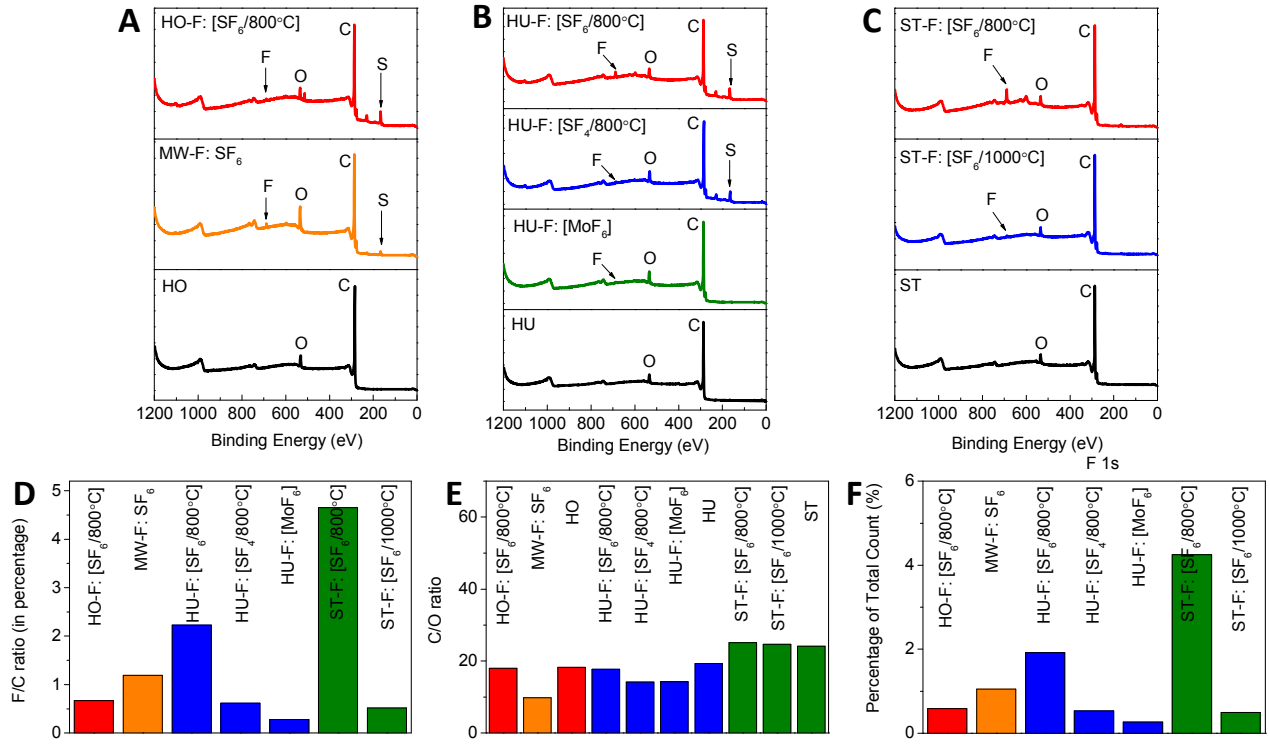

Figure 3. Wide-scan XP spectra of fluorinated graphenes.

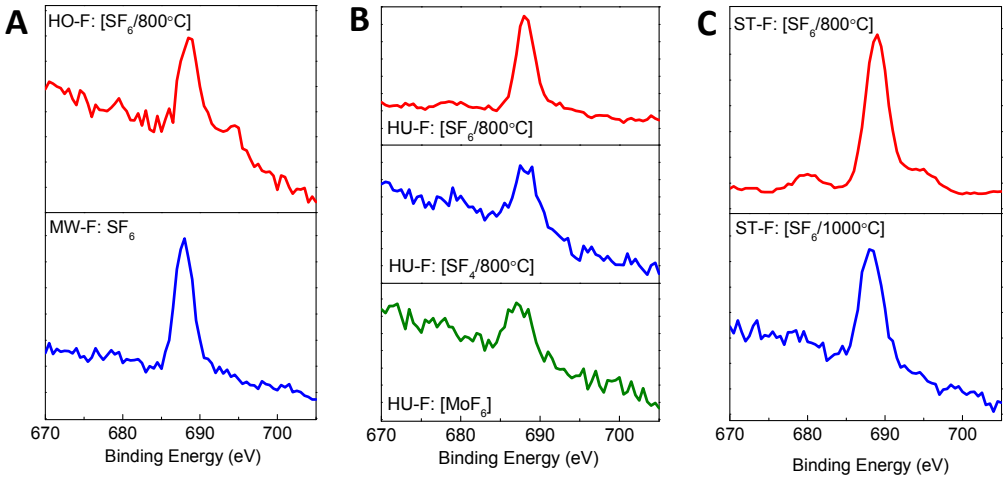

Figure 4. High-resolution XPS of fluorinated graphenes at energy of F1s.

Table 1. Composition of fluorinated graphenes based on combustible elemental analysis.

Sample	At. % N	At. % C	At. % H	At. % F	At. % O
HO-F: [SF_6/800°C]	0.05	76.52	1.14	1.45	20.84
HU-F: [SF_4/800°C]	0.05	77.40	4.50	2.04	16.00
HU-F: [SF_6/800°C]	0.02	75.88	1.64	1.80	20.66
ST-F: [SF_6/1000°C]	0.02	91.84	0.24	0.92	6.98
ST-F: [SF_6/800°C]	0.57	80.33	1.86	2.40	14.84
HU-F: [MoF_6]	0.00	74.87	6.57	0.84	17.72
MW-F: [SF_6]	0.06	85.49	2.90	1.47	10.09

The difference between HO, HU and ST graphite oxide is not only in C/O ratio, but also in the type of oxygen containing groups they contain. We have demonstrated this before.[25] We have also showed that type of graphite oxide directly influence doping graphene with sulphur[10] or hydrogenation of the material.[26]

A high-resolution XPS (HR-XPS) scan was also performed for the specific electronic state of the element of interest. We have measured the HR-XPS for F 1s (Figure 4) and C 1s (Figure S3) to investigate the various bond interactions present for each element. All fluorinated materials displayed a single and symmetrical F 1s peak at approximately 688 eV binding energy as observed in Figure 4, A for fluorinated HO materials; Figure 4, B for fluorinated HU materials; and Figure 4, C for fluorinated ST materials. F 1s peak at similar binding energy was previously observed in other works.[14]

In the HR-XPS spectra of the various materials (as shown in Figure S-3, A, B and C), further processing of the results obtained were performed to gain insights on the bond interactions of C 1s. Relative sensitivity factors were taken into considerations during careful fitting of the high-resolution XPS spectrum. Fitting of the XPS spectra was executed to investigate the different types of bonding interactions that existed for the electronic state of a specific element. The fitted results are as observed in Figure S-3, A for HO materials, B for HU materials and C for ST materials where spectra of fluorinated and non-fluorinated standards (HU, HO and ST) are included for comparison. The C 1s spectra of all standards consists of C=C at 284.5 eV, C-C at 285.7 eV, C-O at 286.7 eV, C=O at 288.0 eV, O-C=O at 289.0 eV and π*-π* at 290.5 eV. The percentages for each bond type of the individual materials are as tabulated in Table S-2 (Supporting Information). All fluorinated materials possess almost all the standard non-fluorinated C 1s bond types as

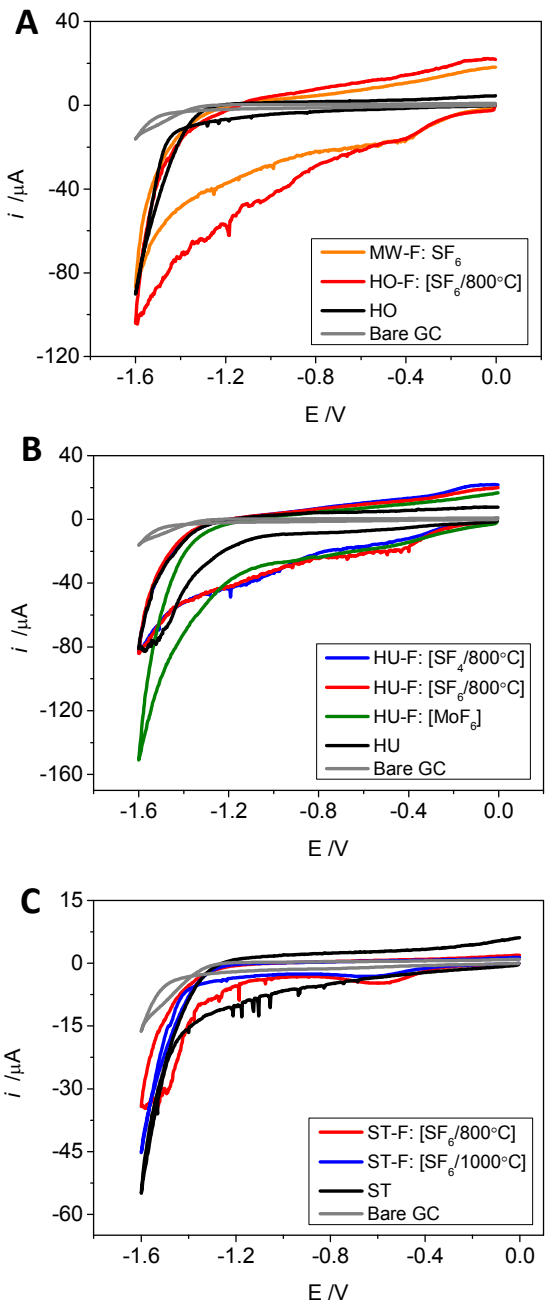

Figure 5. Inherent electrochemistry of fluorinated graphenes. Conditions: phosphate buffer, 50 mM, pH 7.2; scan rate 100 mV/s.

mentioned above with the absence of a few bond interactions (refer to Table S-2). However, the appearance of some C-F bonds was observed for all the fluorinated materials such as C-CF at 286 eV, C_{sp2}-F at 288.0 eV, C-F at 288.5 eV, C-F_2 at 291 eV where the various percentages of abundance are calculated and presented in Table S-2. The presence of such C-F interactions was also previously reported in literature where studies were performed on graphene materials after fluorination treatments.[14-23] As observed in Table S-2, it can be concluded that the amount of C=C interactions decrease after fluorine treatments which indicates that fluorination depletes sp^2 C=C bonds.

Electrochemistry can provide further insight into two main characteristics of resulting materials. First, it is possible to evaluate presence of peroxy, aldehyde and expoxy groups by using cyclic voltammetry; second, it is possible to determine heterogeneous electron transfer rates of the resulting materials, which is crucial for their applications in electrochemical devices. To the point (i), the presence of oxygen containing groups on the surface of the materials can also be explored through the execution of CV in deoxygenated phosphate buffer solution (PBS). It was previously known that aldehyde, peroxy and epoxy groups in graphene oxide undergo chemically irreversible reduction.[27] Cyclic voltammograms of the materials are as shown in Figure 5 where the results are obtained under room temperature conditions with a pH7.4 deoxygenated PBS. The CV results show that HU-F: [SF_6/800°C], HU-F: [SF_4/800°C], HU-F: [MoF_6] and HU display no reduction peaks between 0 V and -1.6 V (refer to Figure 5, B). This results support the earlier observation in XPS where all materials have extremely high C/O ratios, indicating the presence of low amounts of oxygen containing groups. The materials of interest were also compared against another standard, unmodified bare glassy carbon (GC) electrode. Bare GC also expectedly exhibited no reduction peaks in deoxygenated PBS. HO materials were also examined using CV technique as shown in Figure 5, A where HO-F: [SF_6/800°C], HO and bare GC show no visible reduction peaks. Similarly, fluorinated microwave graphene did not display a reduction peak from 0 V to -1.6 V during the CV scan. This result was expected as earlier XPS findings have shown that all HU materials have almost similar C/O ratios as the HO materials. All fluorinated and non-fluorinated ST materials (refer to Figure 5, C) has also shown no reduction peaks at all during CV scans. This was anticipated as all ST materials have the highest C/O ratios as compared to HU and HO materials hence, the least amount of oxygen functionalities on the surface.

The heterogeneous electron transfer (HET) rate of the materials were also investigated with CV methods in ferrocyanide solution ($[Fe(CN)_6]^{3-}$) where the peak-to-peak separation ($\Delta E_{p\text{-}p}$) of each material can be examined (Figure 6). The calculated $\Delta E_{p\text{-}p}$ values are 147 mV for HU-F: [SF_6/800°C], 127 mV for HU-F: [SF_4/800°C], 151 mV for HU-F: [MoF_6] and 149 mV for HU. Bare GC has the largest peak-to-peak separation of 300 mV and hence, the slowest HET rate at the surface of the material. HO-F: [SF_6/800°C], HO and fluorinated microwave graphene have $\Delta E_{p\text{-}p}$ values of 117 mV, 142 mV and 125 mV respectively. Similar calculations were also performed for ST materials where ST-F: [SF_6/800°C] has a value of 154 mV, ST-F: [SF_6/1000°C] has a value of 188 mV and ST has a value of 156 mV. It was observed that bare GC has the widest peak separation among all the materials that were compared. It can also

be concluded that most GOs flurorinated with SF_6 at 800°C have the smallest peak-to-peak separation as compared to their fluorinated counterparts. The HET rates (k^0_{obs}) were then calculated using the Nicholson approach where $\Delta E_{p\text{-}p}$ is related to a dimensionless parameter Ψ which is eventually related to k^0_{obs}. The calculated

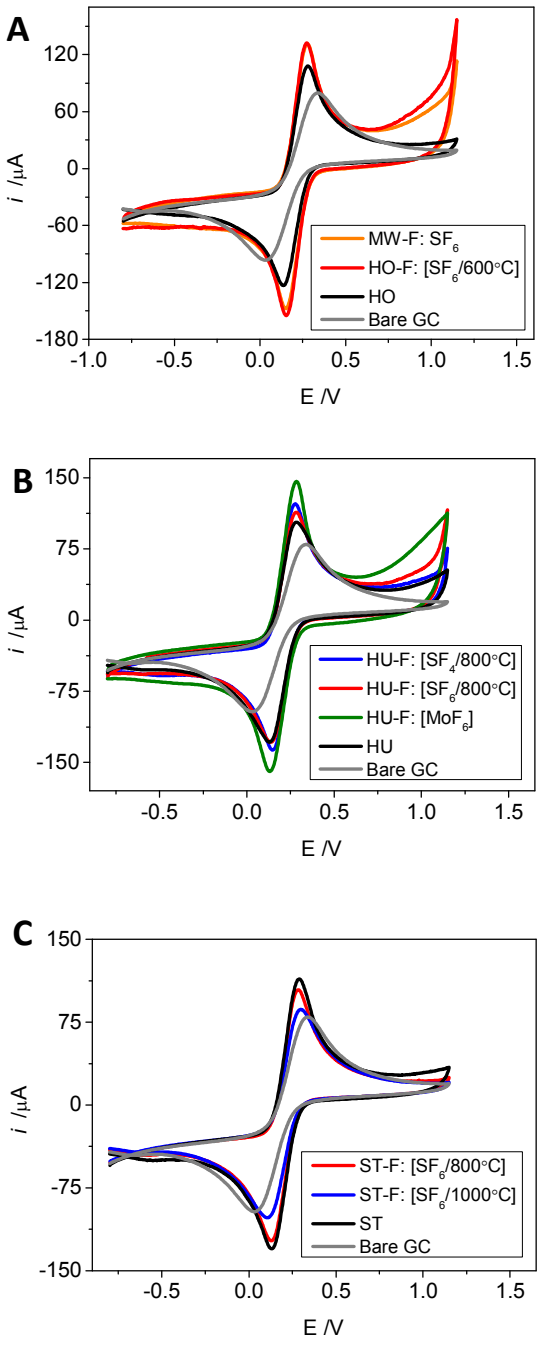

Figure 6. Heterogeneous electron transfer at fluorinated graphenes. Conditions: phosphate buffer, 50 mM, pH 7.2; scan rate 100 mV/s; 10 mM ferro/ferrricyanide as depolarizer.

values are 2.27 x 10^{-3} cm s^{-1} for HU-F: [SF_6/800°C], 2.97 x 10^{-3} cm s^{-1} for HU-F: [SF_4/800°C], 2.13 x 10^{-3} cm·s^{-1} for HU-F: [MoF_6] and 2.20 x 10^{-3} cm s^{-1} for HU. HO-F: [SF6/800°C] and HO were found to possess 3.39 x 10^{-3} cm s^{-1} and 2.43 x 10^{-3} cm s^{-1} respectively. Fluorinated microwave graphene has a value of 3.07 x 10^{-3} cm s^{-1}. ST-F: [SF6/800°C] has a value of 2.06 x 10^{-3} cm s^{-1} while ST-F: [SF6/1000°C] has a value of 1.29 x 10^{-3} cm s^{-1}. The standard unfluorinated ST material has a HET value of 1.99 x 10^{-3} cm s^{-1} while bare GC has a value of 2.82 x 10^{-4} cm s^{-1}. As expected, bare GC has the slowest electron transfer rate at the surface as compared to all the materials studied. Among the fluorinated materials, fluorinated microwave graphene has the fastest HET rate followed by materials that are fluorinated with SF_6 at 800°C. There is general trend where electrochemical performance increases with increased fluorination within the type of graphite oxide precursor. The observed deviations may be hypothesized to be caused by different topology of fluorination - fluoronated graphene lead into the creation of islands in the graphene lattice, as shown recently.[28]

Conclusion

We have successfully demonstrated the fluorination of graphene using reagents such as SF_6, SF_4 and MoF_6. The materials obtained are then extensively studied through various characterization techniques such as XPS, Raman spectroscopy, electrochemistry and combustible elemental analysis to investigate their properties. The use of SF_6 as fluorination agent at 800°C have produced the highest fluorine content as compared to other fluorine sources. The presence of fluorine content as high as 4.25% has also resulted in interesting properties such as fast electron transfer rates at the material's surface which has important implications for future electrochemical applications.

Experimental Section

Materials

Sulphuric acid (98 %), nitric acid (fuming, 98 %), nitric acid (68%), potassium chlorate (98 %), hydrochloric acid (37 %), sodium nitrate (99.5%), potassium permanganate (99%), hydrogen peroxide (30%), silver nitrate (99.5 %) and barium nitrate (99.5 %) were obtained from PENTA, Czech Republic. Graphite microparticles (2-15 μm, 99.999%) were obtained from Alfa Aesar, Germany. Nitrogen (99.9999% purity) and sulfur hexafluoride (99.95% purity) were obtained from SIAD, Czech Republic. Sulfur tetrafluoride (99% purity) was obtained from Matheson, USA and molybdenum hexafluoride (99.9% purity) from Fluka, Switzerland. Potassium ferrocyanide, N,N-dimethylformamide (DMF), potassium phosphate dibasic, sodium phosphate monobasic, potassium chloride, sodium phosphite dibasic pentahydrate and sodium chloride were obtained from Sigma-Aldrich, Singapore. Deionized water was used for the preparation of the electrolytes that were used in all the electrochemical measurements. Glassy carbon working electrode (GC), platinum auxiliary electrode (Pt) and Ag/AgCl reference electrode were purchased from Autolab, The Netherlands.

Apparatus

JEOL 7600F field-emission scanning electron microscope, Japan was used to obtain SEM images. The samples were affixed onto the sample stub with a conductive carbon tape. The XPS and HR-XPS measurements were acquired with a Phoibos 100 spectrometer and a monochromatic Mg X-ray radiation source (SPECS, Germany). All measurements were executed with a 12.53 kV X-ray source. A XPS sample holder and a sticky conductive carbon tape was used to attach the XPS samples. A homogeneous and uniform layer of the material was attached onto the tape before the sample was loaded into the XPS chamber for a measurement. Confocal micro-Raman LabRam HR instrument (Horiba Scientific) in backscattering geometry with a CCD detector was used for Raman spectroscopic measurements. Silicon wafer was utilized for calibration at 0 cm^{-1} and 520 cm^{-1} to give a peak position resolution of less than 1 cm^{-1}. A 514.5 nm Ar laser, an Olympus optical microscope and a 100x objective lens was used for all the measurements. All materials were well-compressed and compacted prior to any measurement. Combustible elemental analysis (CHNS-O) was performed with a PE 2400 Series II CHNS/O Analyzer (Perkin Elmer, USA). In CHN operating mode (the most robust and interference free mode), the instrument employs a classical combustion principle to convert the sample elements to simple gases (CO_2, H_2O and N_2). The PE 2400 analyzer performs automatically combustion and reduction, homogenization of product gases, separation and detection. A microbalance MX5 (Mettler Toledo) is used for precise weighing of samples (typically 1.5 – 2.5 mg per single sample analysis). The accuracy of CHN determination is better than 0.30% abs. Internal calibration is performed using N-phenyl urea. Electrochemical voltammetric measurements were performed using a microAutolab Type III electrochemical analyzer (Eco Chemie, The Netherlands) and a NOVA 1.7 software (Eco Chemie). Nova 1.7 software was published by Metrohm Autolab B.V. in support of Metrohm Autolab's potentiostat/galvanostat equipment. The micro-photoluminescence spectra were measured using Renishaw In-Via confocal Raman microscope. For the measurement were used He-Cd laser (325 nm, 22 mW) and DPSS laser (532 nm, 50 mW). The measurement was performed with a 40x UV objective and 50x VIS-NIR objective. Silicon wafer was utilized for calibration at 0 cm^{-1} and 520 cm^{-1} Raman shift for both lasers to give a peak position resolution of less than 1 cm^{-1}. The UV-VIS absorbance spectra were measured in 200 - 1100 nm range using Cary 50 spectrometer (Agilent, USA). For the measurement the suspension in hexane were prepared by ultrasonication (400 W, 10 minutes, 1 mg/mL).

Synthesis procedure of Hofmann graphite oxide.[29] Graphite oxide preparation with the Hoffman method: 87.5 mL of sulphuric acid (98 % concentration) and 27 mL of nitric acid (68 %) were added to a reaction flask containing a magnetic stir bar. The mixture was subsequently cooled to 0 °C and 5 g of graphite was added. The mixture was then vigorously stirred to avoid agglomeration and to obtain a homogeneous dispersion. While keeping the reaction flask at 0 °C, 55 g of potassium chlorate was slowly added to the mixture. Upon completion dissolution of the potassium chlorate, the reaction flask was then left loosely capped to allow the gas evolved during the reaction to escape. The mixture was then continuously stirred for 72 h at room temperature. Upon completion of the reaction, the mixture was poured into 3 L of deionized water and decanted. Graphite oxide was then redispersed in HCl (5 %) solutions to remove sulphate ions and repeatedly centrifuged and redispersed in deionized water until a negative reaction on chloride and sulphate ions (with $AgNO_3$ and $Ba(NO_3)_2$ respectively) was achieved. Graphite oxide slurry was then dried in a vacuum oven at 50 °C for 48 h before use.

Synthesis procedure of Hummers graphite oxide.[30] Graphite oxide preparation with the Hummeers method: 115 ml of sulfuric acid (98%) was cooled to 0 °C and then 5 g of graphite and 2.5 g of $NaNO_3$ were added to the mixture. While vigorously stirred, 15 g of $KMnO_4$ were added over a period of two hours. The reaction mixture was then removed from the cooling bath and stirred at room temperature for 4 hours. The reaction mixture was then heated to 35 °C for 30 minutes, poured into 250 ml of deionized water and heated to 70 °C. After 15 minutes the mixture was poured into 1 L of deionized water. Unreacted $KMnO_4$ was decomposed with 10% hydrogen peroxide. The reaction mixture was then decanted and repeatedly centrifuged and re-dispersed until a negative reaction for sulfate ions (with $Ba(NO_3)_2$) was achieved. Graphite oxide slurry was then dried in a vacuum oven at 60 °C for 48 hours before further use.

Synthesis procedure of Staudenmaier graphite oxide.[31] Graphite oxide preparation with the Staudenmaier method: 87.5 ml of sulfuric acid (98 %) and 27 ml of nitric acid (98 %) were first cooled to 0 °C before 5 g of graphite were added to the mixture. The reaction mixture was then intensively stirred while 55 g of potassium chlorate were added over a period of 30 minutes. The reaction flask was then loosely capped to allow the escape of chlorine dioxide gas. The mixture was continuously stirred for 96 hours at room temperature and then poured into 3 L of deionized water. After decantation, the graphite oxide was re-dispersed in 5 % hydrochloric acid. The graphite oxide was decanted from hydrochloric acid and repeatedly centrifuged and re-dispersed until a negative reaction for chloride and sulfate ions (with $Ba(NO_3)_2$ and $AgNO_3$) was observed. Graphite oxide slurry was finally dried in a vacuum oven at 60 °C for 48 hours before further use.

Synthesis procedure of fluorine doped graphene–thermal exfoliation. All of the fluorine-doped graphene were exfoliated in the same reactor as the thermally reduced graphene oxides. For every reaction, 100 mg of the graphite oxide starting material were inserted into a quartz glass capsule covered by sintered quartz glass filter facing the direction of the gas flow. The capsule was then attached to a magnetic manipulator and placed into a quartz horizontal reactor in the furnace. Before the placement of the sample into the hot zone of the reactor, the whole system was repeatedly evacuated and filled up with nitrogen. A pure fluorine

precursor was used in the case of SF_4 and SF_6. The mixture of nitrogen and fluorine precursor was used for the fluoration process with MoF_6. First, the fluorine precursor flow (0.5 L/min) was stabilized for 5 minutes. For the fluoration with MoF_6 were used the mixture of MoF_6 gas (0.3 L/min) and nitrogen (1 L/min). The temperature of exfoliation was 800 °C and 1000 °C respectively. Then the capsule with the sample was inserted into the furnace for 12 minutes and pulled out again at the end of the reaction. The 12 minutes exposure of graphene at these conditions led to a complete exfoliation and fluoration. All exfoliation steps were performed under atmospheric pressure.

Synthesis procedure of fluorine doped graphene–microwave plasma exfoliation:

Synthesis of fluorinated graphene in microwave SF_6 plasma: The synthesis of fluorine doped graphene was performed in low pressure fluorine microwave plasma generated from SF_6. The graphite oxide prepared according to Hofmann method was placed inside a quartz glass reactor which was evacuated and flushed with nitrogen. At the base pressure of 1 mbar, the SF_6 gas was introduced inside quartz glass reactor (0.1 L/min, 5 mbar) and the graphite oxide was exfoliated by applying microwave radiation for 30 s (1 kW, 2.45 GHz). The exfoliation procedure was accompanied by the increase of the pressure to about 20 mbar. The reactor was again evacuated and flushed with the sulfur hexafluoride gas (0.1 L/min) to remove the exfoliation byproducts and at the pressure of 5 mbar and continual flow of SF_6 the microwave radiation was applied for 3 minutes. Application of microwave radiation on SF_6 at reduced pressure led to the formation of fluorine plasma.

Cyclic Voltammetry

The glassy carbon electrodes were cleaned by polishing with alumina suspension to renew the electrode surface then washed and wiped dry prior to use. The materials were dispersed in DMF as the solvent to obtain a 1.0 $mg{\cdot}mL^{-1}$ suspension. The suspension was then sonicated for 5 minutes at room temperatures before each use. A cleaned GC electrode was then modified by coating with a 1 µL aliquot of the suspension and left to dry under a lamp to give a layer of randomly dispersed material. The modified GC electrodes, Ag/AgCl reference electrode, and Pt counter electrode were then placed into an electrochemical cell which contains the electrolyte and the scans were then performed. The electrolytes used were 50 mM pH7.4 deoxygenated phosphate buffer solution (PBS) and 10 mM Ferro/Ferricyane dissolved in PBS. All measurements were performed for two consecutive scans at a scan rate of 100 mV s^{-1} where three measurements were carried out for each material and also for each electrolyte. The deoxygenation of the 50 mM pH7.4 PBS was achieved by bubbling nitrogen gas into the PBS for 15 minutes before each use.

Acknowledgements

M.P. acknowledges Tier 2 grant (MOE2013-T2-1-056; ARC 35/13) from Ministry of Education, Singapore. Z.S. and O.J. was supported by Specific university research (MSMT 20/2013).

Notes and references

* - corresponding author
[a]*Division of Chemistry & Biological Chemistry*
School of Physical and Mathematical Sciences
Nanyang Technological University
Singapore 637371
Fax: (65) 6791-1961
E-mail: pumera@ntu.edu.sg

[b]*Department of Inorganic Chemistry, Institute of Chemical Technology, Technická 5, 166 28 Prague 6, Czech Republic*
E-mail: zdenek.sofer@vscht.cz

1 K. S. Novoselov, A. K. Geim, S. V. Morozov, D. Jiang, Y. Zhang, S. V. Dubonos, I. V. Grigorieva, A. A. Firsov, *Science,* 2004, **306**, 666; A. K. Geim, K. S. Novoselov, *Nat. Mater.,* 2007, **6**, 183; J. A. Rogers, *Nat. Nanotechnol.,* 2008, **3**, 254; M. D. Stoller, S. Park, Y. Zhu, J. An, R. S. Ruoff, *Nano Lett,.* 2008, **8**, 3498; Z. Liu, J. T. Robinson, X. Sun, H. Dai, *J. Am. Chem. Soc.,* 2008, **130**, 10876.
2 M. Pumera, *Chem. Soc. Rev.,* 2010, **39**, 4146.
3 A. Bonanni, A. H. Loo, M. Pumera, *Trends Anal. Chem.,* 2012, **37**, 12.
4 C. N. R. Rao, A. K. Sood, K. S. Subrahmanyam, A. Govindaraj, *Angew. Chem., Int. Ed.,* 2009, **48**, 7752.
5 H. L. Poh, P. Šimek, Z. Sofer, M. Pumera, *Chem. Eur. J.,* 2013, **19**, 2655.
6 H. L. Poh, P. Šimek, Z. Sofer, I. Tomandl, M. Pumera, *J. Mater. Chem. A,* 2013, **1**, 13146.
7 M. Pumera, C. H. A. Wong, *Chem. Soc. Rev.,* 2013, **42**, 5987.
8 M. Seredych, T. J. Bandosz, *J. Mater. Chem. A*, 2013, **1**, 11717.
9 Z. Yang, Z. Yao, G. Li, G. Fang, H. Nie, Z. Liu, X. Zhou, X. Chen, S. Huang, *ACS Nano*, 2012, **6**, 205.
10 H. L. Poh, P. Šimek, Z. Sofer, M. Pumera, *ACS Nano*, 2013, **7**, 5262.
11 Y. Zheng, Y. Jiao, L. Ge, M. Jaroniec, S. Z. Qiao, *Angew. Chem. Int. Ed*., 2013, **52**, 3110.
12 C. H. Choi, M. W. Chung, H. C. Kwon, S. H. Park, S. I. Woo, *J. Mater. Chem. A,* 2013, **1**, 3694.
13 D. Sen, K. S. Novoselov, P. M. Reis, & M. J. Buehler, *Small,* 2011, **6**, 1108.
14 K.-J. Jeon, Z. Lee, E. Pollak, L. Moreschini, A. Bostwick, C.-M. Park, R. Mendelsberg, V. Radmilovic, R. Kostecki, T. J. Richardson, E. Rotenberg, ACS Nano 2011, 5, 1042.
15 Q. Feng, N. Tang, F. Liu, Q. Cao, W. Zheng, W. Ren, X. Wan, Y. Du, *ACS Nano,* 2013, **7**, 6729.
16 W.-K. Lee, J. T. Robinson, D. Gunlycke, R. R. Stine, C. R. Tamanaha, W. P. King, P. E. Sheehan, *Nano Lett.,* 2011, **11**, 5461.
17 V. Wheeler, N. Garces, L. Nyakiti, R. Myers-Ward, G. Jernigan, J. Culbertson, C. Eddy Jr., D. K. Gaskill, *Carbon,* 2012, **50**, 2307.
18 K. Tahara, T. Iwasaki, A. Matsutani, M. Hatano, *Applied Phys. Lett.,* 2012, **101**, 163105.

19 H. Yang, M. Chen, H. Zhou, C. Qiu, L. Hu, F. Yu, W. Chu, S. Sun, L. Sun, *J. Phys. Chem. C,* 2011, **115**, 16844.
20 W. H. Lee, J. W. Suk, H. Chou, J. Lee, Y. Hao, Y. Wu, R. Piner, D. Akinwande, K. S. Kim, R. S. Ruoff, *Nano Lett.* 2012, **12**, 2374.
21 M. Chen, H. Zhou, C. Qiu, H. Yang, F. Yu, L. Sun, *Nanotechnology,* 2012, **23**, 115706.
22 X. Yu, K. Lin, K. Qiu, H. Cai, X. Li, J. Liu, N. Pan, S. Fu, Y. Luo, X. Wang, *Carbon*, 2012, **50**, 4512.
23 B. Wang, J. Wang, J. Zhu, *ACS Nano* **2014**, in press, DOI: 10.1021/nn406333f
24 L. G. Canado, K. Takai, T. Enoki, M. Endo, Y. A. Kim, H. Mizusaki, A. Jorio, L. N. Coelho, R. Magalhaes-Paniago, M. A. Pimenta, *Appl. Phys. Lett.* **2006**, *88*, 163106.
25 C. K. Chua, Z. Sofer, M. Pumera, *Chem Eur. J.* 2012, **18**, 13453.
26 A. Y. S. Eng, H. L. Poh, F. Sanek, M. Marysko, S. Matejkova, Z. Sofer, M. Pumera, *ACS Nano* 2013, **7**, 5930.
27 E. L. K. Chng, M. Pumera, *Chem. Asian J.* 2011, **6**, 2850.
28 B. Wang, J. Wang, J. Zhu, ACS Nano 2014, 8, 1862
29 Hofmann, U.; Konig, E. *Z. Anorg. Allg. Chem.* 1937, **234**, 311.
30 Hummers, W. S.; Offeman, R. E. *J. Am. Chem. Soc.* 1958, **80**, 1339.
31 Staudenmaier, L. *Ber. Dtsch. Chem. Ges.* 1898, **31**, 1481.

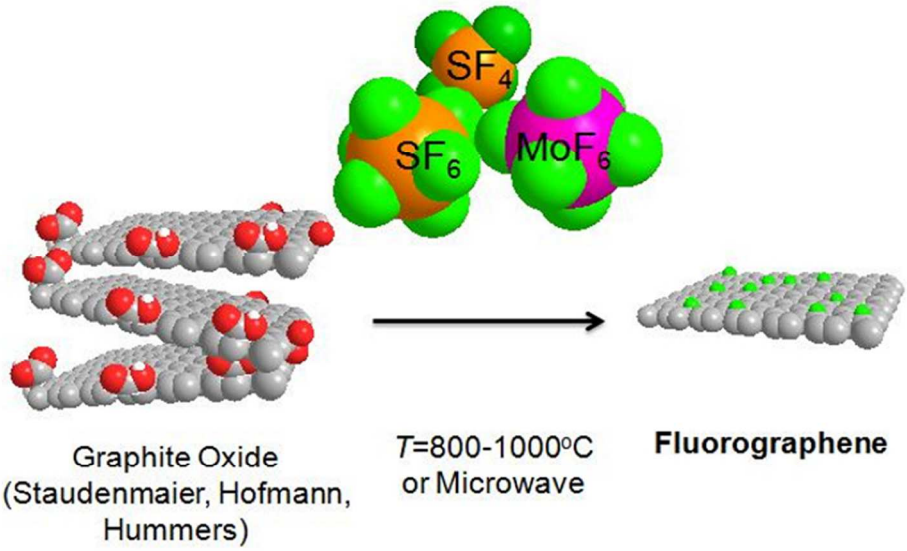

63x39mm (300 x 300 DPI)